JOURNAL OF Applied Polymer SCIENCE

Grafting Modification of Electrospun Polystyrene Fibrous Membranes via an Entrapped Initiator in an Acrylic Acid Aqueous Solution

Ran Tao,[1] Xinsheng Zhu,[1,2] Yu-Ting Zuo,[1] Li-Juan Fan,[3] Bing Wang,[1] Ji-Ting Xin[1]

[1]Faculty of Textile and Clothing Engineering, Soochow University, 178 Eastern Ganjiang Road, Suzhou, Jiangsu 215021, People's Republic of China

[2]National Engineering Laboratory for Modern Silk, Soochow University, 199 Ren'ai Road, Suzhou, Jiangsu 215123, People's Republic of China

[3]College of Chemistry, Chemical Engineering and Materials Science, Soochow University, 199 Ren'ai Road, Suzhou, Jiangsu 215123, People's Republic of China

Correspondence to: X. Zhu (E-mail: zhuxinsheng@suda.edu.cn) or L.-J. Fan (E-mail: ljfan@suda.edu.cn)

ABSTRACT: Ultrafine electrospun polymer fibers, with their large specific surface areas, have not found wide applications partly because the fiber surfaces usually carry an insufficient quantity of active groups. The electrospinning and surface-grafting copolymerization of polystyrene fibrous membranes were carried out via the embedded radical initiator approach. The results from X-ray photoelectron spectroscopy show that the initiator added to the polystyrene dope was deliberately expelled onto the fiber surfaces. The microstructure and hydrophilicity of the grafted membranes were investigated with Fourier transform infrared spectroscopy, scanning electron microscopy, and water contact angle and water uptake capacity measurements. An increase in the initiator dosages led to decreases in the grafting rate, water uptake, and hydrophilicity of the grafted membranes; the opposite was true for increases in the neutralization of acrylic acid (AA). However, the grafting, water uptake, and hydrophilicity of the grafted membranes presented nonlinear relationships with the concentration of AA. The initiator emigration technique will provide a facile and feasible platform for the surface-grafting modification of electrospun membranes. © 2012 Wiley Periodicals, Inc. J. Appl. Polym. Sci. 000: 000–000, 2012

KEYWORDS: crosslinking; graft copolymers; membranes; polystyrene

Received 15 November 2011; accepted 10 January 2012; published online 00 Month 2012
DOI: 10.1002/app.36797

INTRODUCTION

Electrospinning is a simple and versatile technique for preparing polymer fibers with diameters ranging from 10s of nanometers to micrometers with very high electrostatic fields. The outstanding properties of the resulting fibrous mats make them favorable candidates for use in many areas, including tissue engineering scaffolds,[1] affinity membranes,[2] filtration,[3] catalysis,[4] and sensors.[5] Electrospun polymer fiber surfaces are often expected to bear some functional groups for most applications. However, only very few polymers carrying active groups can be directly electrospun because the pendant active groups often present physicochemical interactions that are too strong for them to be well dissolved. The introduction of reactive groups, such as carboxyl, amine, and amide groups, onto chemically inert polymer fiber surfaces is a necessary step in these applications. An aminated electrospun polyacrylonitrile nanofiber was produced by the functionalization of the fiber with diethylenetriamine; this resulted in adsorptive fibrous mats.[6] A biocatalyst with a high activity retention of *Candida rugosa* lipase was fabricated by the covalent immobilization of lipase on a cellulose nanofiber membrane via sequential steps: the electrospinning of cellulose acetate, hydrolysis under alkaline conditions, oxidation with sodium periodate, and finally, coupling with the lipase.[7] Reactive ultrafine fiber support materials were successfully made by the copolymerization of styrene and maleic anhydride followed by electrospinning and, finally, hydrolysis under a dilute alkaline aqueous solution.[8] β-Cyclodextrin containing polystyrene nanofibers, mainly on fiber surfaces, were successfully electrospun.[9] Improved cell attachment and proliferation of the electrospun poly(ϵ-caprolactone) nanofibrous membrane were realized through alkaline treatment.[10]

Different methods, such as plasma pretreatment[11,12] and ultraviolet (UV)-, plasma-, and γ irradiation-induced grafting copolymerization,[13,14] have been used to surface-modify polymers to improve their electrospun fibrous applicability. Cold plasma treatment significantly altered the surface wettability of polyamide 6 nanofibers.[11] A cell adhesion and proliferation

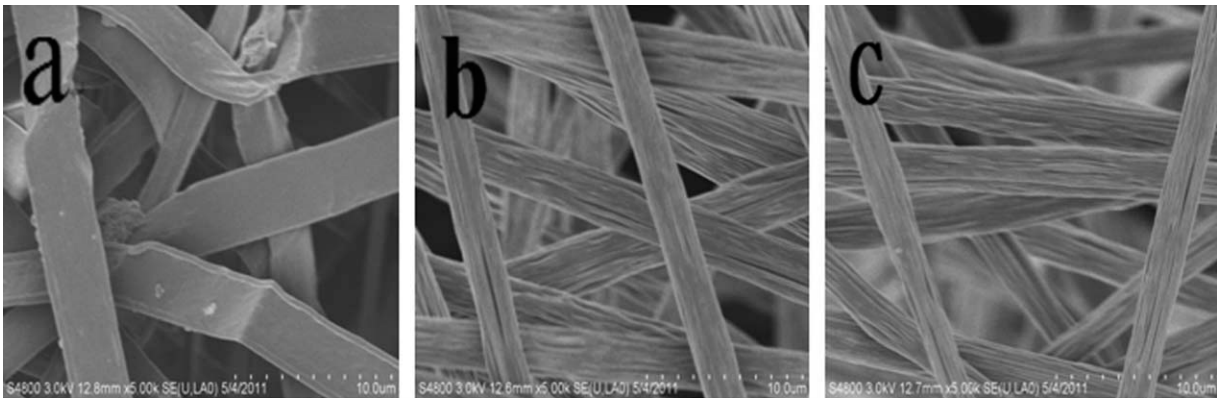

Figure 1. SEM images of the membranes spun at different temperatures and humidities: (a) 293 K and 20% RH, (b) 293 K and 80% RH, and (c) 298 K and 80% RH.

experiment of three model cells, fibroblasts, chondrocytes, and osteoblasts, verified that oxygen- and argon-plasma treatments of electrospun polycaprolactone nanofiber meshes were successful.[12] Electrospun poly(vinylidene fluoride-*co*-hexafluoropropylene) fibrous membranes were subjected to plasma pretreatment followed by UV-induced surface grafting and quaternization and were highly effective against both Gram-positive staphylococcus aureus and Gram-negative *Escherichia coli* bacteria.[13] The surface of electrospun poly(vinylidene) fluoride nanofibrous membranes was exposed to argon plasma and subsequently copolymerized with methacrylic acid (MAA), and the results indicate that the grafted membranes could be engineered through surface modification to achieve small pores while retaining their high flux performance.[14] Carboxyl groups were introduced onto polysulfone fiber surfaces through grafting copolymerization after an air-plasma pretreatment.[2] After electrospun biodegradable polyesters nanofibrous scaffolds were treated with oxygen plasma, the hydrophilic functional groups were successfully grafted onto fiber surfaces; this resulted in a significant improvement in cell attachment and proliferation.[15] The regulation of cell–material interactions was manipulated by the grafting copolymerization of acrylic acid (AA) after the electrospun poly(L-lactide-*co*-ϵ-caprolactone) fibrous membranes were treated with γ-ray irradiation, and Arg–Gly–Asp (RGD)-containing peptides were subsequently immobilized for tissue engineering applications.[16]

However, for the surface modification of polymer nanofibers, harsh reaction conditions, such as those with irradiation and plasma, are to be avoided because ultrafine polymeric nanofibers are usually not as strong as bulk materials and can be easily destroyed.[17] The Ce(IV)-induced graft copolymerization of MAA (MBPO) on electrospun poly(ethylene terephthalate)[17] and polysulfone fiber surfaces[18] were implemented after the fibers were pretreated by a formaldehyde solution. Recently, Liu et al.[19] put forward the concept of tunable surface chemistry for the functionalization of electrospun nanofibrous membranes, in which the combination of the embedded initiator and the subsequent surface-initiation polymerization was done as a platform for extending the application of the electrospun nanofibers.

In fact, the surface morphology of electrospun fibers is often affected by many processing parameters, such as the solvent and ambient humidity.[20–24] At high relative humidity (RH), the

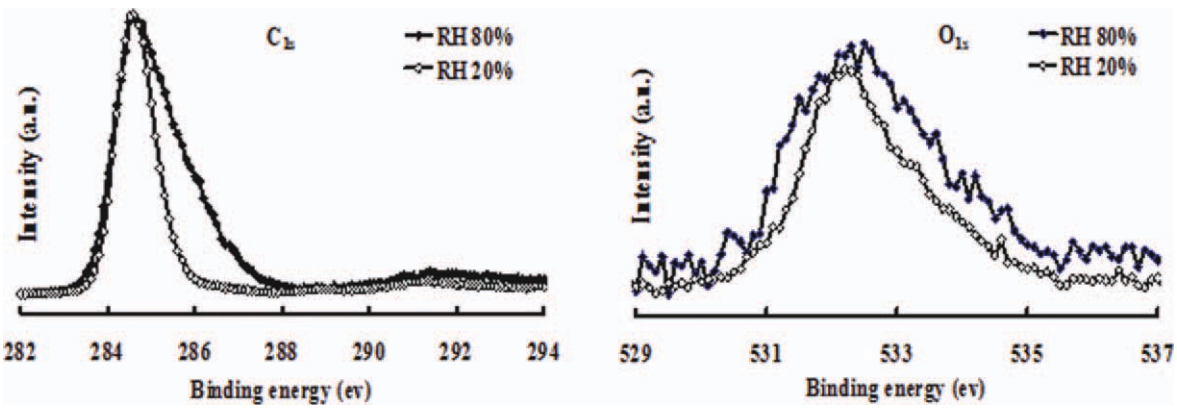

Figure 2. XPS spectra of C_{1s} and O_{1s} of the membranes spun at different humidities. [Color figure can be viewed in the online issue, which is available at wileyonlinelibrary.com.]

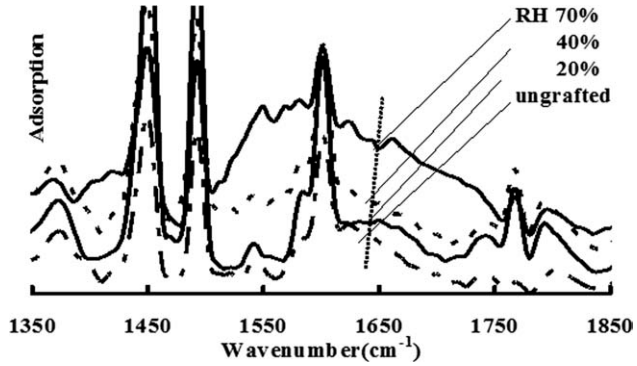

Figure 3. IR spectra of the grafted membranes spun at different humidities.

moisture in air may be condensed on the fiber surface,[22] and somehow, the evaporation of the solvent and the formation of micropores are strongly related to ambient humidity. At low RH, the rapid evaporation of the solvent causes the clogging of the spinet tip and the formation of ribbonlike fibers.[25]

In this study, a free-radical initiator was added while a polystyrene dope was made with butanone. The initiator was induced toward the fiber surfaces during electrospinning via the regulation of RH, and subsequently, poly(acrylic acid) was grafted onto the electrospun membranes in an aqueous solution. The entrapment of the initiator within electrospun polymer fibers really provided a facile way to create functional polymer ultrafine fibers and may find wide potential application in the fabrication of functional electrospun fiber surfaces.

EXPERIMENTAL

Raw materials

The deionized water, butanone, sodium hydroxide, and benzoyl peroxide (BPO) used in this study were analytical grade. AA (BPO) was chemically pure and was vacuum-distilled before use. Polystyrene (PS), with a viscosity-average molar mass of about 350,000 g/mol, was made in our laboratory with emulsion polymerization.

Electrospinning and heat treatment

PS (8% w/v) in a butanone solution with a given amount of the initiator BPO was placed in a syringe connected with a metal needle on which a copper plate (15 mm in diameter and 0.2 mm in thickness) served as an auxiliary electrode and was fixed to converge with an electrospinning jet. The needle was controlled by a syringe pump (W2-50C2-type micropump, Zhejiang University Medical Instrument Co., Ltd., Zhejiang, China) at a constant flow rate of 2.5 mL/h. A high-voltage direct-current power supply (DW-P503-4AC, Tianjin Dongwen High Voltage Power Supply Factory, Tianjin, China) was used to generate a potential difference of 8 kV between the needle and an aluminum grounded collector placed 12 cm from the tip of the needle. All of the experiments were carried out at 25°C, and an RH of 60%, unless otherwise specified, was used. After the electrospinning, the fibrous membranes were removed from the collector and sandwiched between two glass sheets and thermally treated at 45°C for 2 h.

Grafting copolymerization

The monomer BPO was partially and gently neutralized with a sodium hydroxide aqueous solution in ice–water bath. The thermally pretreated electrospun membrane embedded with the initiator BPO was placed into a 250-mL flask containing 100 mL of BPO aqueous solution. The reaction system was vacuumed and filled with nitrogen three times. A small rubber balloon was used to seal the flask to make sure that the pressure inside the flask did not change a lot during the reaction. Then, it was put into an oscillating water bath at 70°C and shaken for about 100 min. Further, the membrane was removed and rinsed with deionized water repeatedly and was finally dried *in vacuo* overnight. Unless specified, the initiator dosage was fixed at 4 wt % PS, the concentration of BPO was 30% v/v, and the neutralization degree of BPO was 60%.

Characterization

Fibrous membrane morphology. Scanning electron microscopy (SEM; Hitachi S-4800 and S-570, Tokyo, Japan) was used to observe the morphology of the PS fiber membranes, and the samples were sputter-coated with gold to prevent charging during SEM imaging.

Microstructural components of the membranes. X-ray photoelectron spectroscopy (XPS; AXIS-Ultra DLD, Shimadzu-Kratos, Lancashire, United Kingdom) was used to determine the enrichment of the initiator on the membrane surface. Monochromatic Al Kα X-rays (1486.7 eV) were used. To compensate for the surface-charging effect, all binding energies were referenced to the C_{1s} hydrocarbon peak at 284.6 eV.

Fourier transform infrared characterization was performed at ambient temperature with a Nicolet 5700 spectrometer (Thermo Electron, Madison, WI) with KBr disc. The samples were pulverized and analyzed with 64 scans at a resolution of 4 cm^{-1} in the range 400–4000 cm^{-1}.

Hydrophilicity of the membrane surface. Water contact angle measurements were performed on membranes with a contact angle meter (contact angle system OCA20, Dataphysics Co., Stuttgart, Germany). A water droplet of 0.2 μL was dispersed on the membrane surface, and the contact angle was determined with the system software.

Water uptake capacity. The membranes were immersed in deionized water at 20°C for 24 h. After the treatment, excess water on the sample surface was wiped with filter paper and weighed. They were dried at 80°C for 2 h and then placed in a desiccator for 48 h to remove residual water and weighed again. The water uptake capacity was determined from the relative weight gain.

Table I. Water Uptake of the Grafted Membranes Spun at Different Humidities

RH during electrospinning (%)	20	60	80
Water uptake (wt %)	710	1550	1510

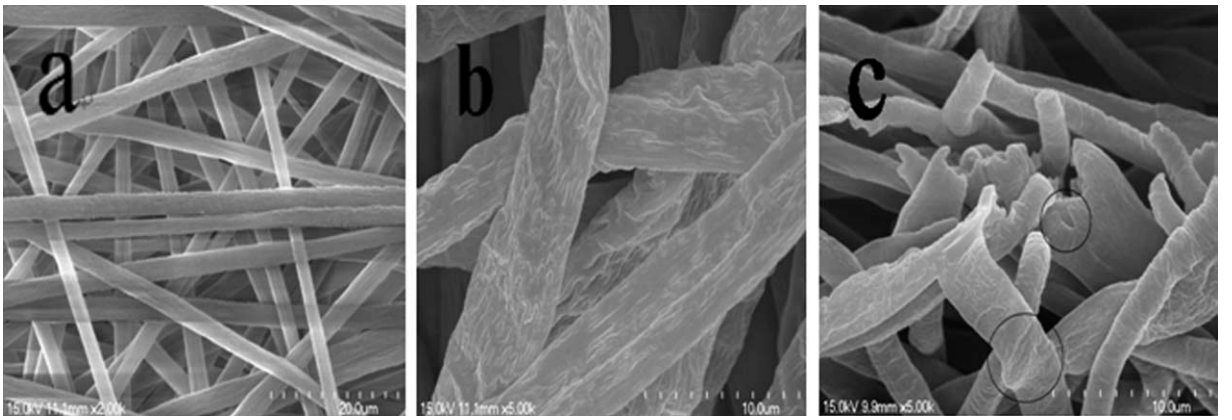

Figure 4. SEM images of the grafted membranes prepared at 60% RH: (a) before grafting and (b,c) after grafting.

RESULTS AND DISCUSSION

Electrospun fiber morphology and emigration of the initiator

Figure 1 presents images of the electrospun fibers at the different RHs and temperatures. A smooth and flat fiber surface was shown when was electrospun at a low RH, whereas there appeared a cucumber-skin structure on the fiber surface at high humidities. The slight difference in ambient temperature did not seem to cause much variation in the fiber appearance. The formation of the smooth ribbonlike fibers could have originated from the spinning jet flight and the hollow-fiber collapse on the collector. It was found that the rapid evaporation of solvent from the flight jet shortened the Newtonian fluid flight phase and quickly moved it into the non-Newtonian whipping region. The extended and violently whipping region may have induced an asymmetric fiber surface structure, with the front surface toward the collector and the rear surface departing from the spinneret tip. On the other hand, the solvent evaporation from the fiber surface was much quicker than that from the inner fiber to the surface area. The continuous solvent evaporation gave rise to the skin–core structured fibers or to hollow fibers after the fibers were deposited on the collector. The hollow fibers finally collapsed into ribbon-structured fibers because of their weight and the pressure difference. However, at high humidities, the slow solvent evaporation extended the Newtonian fluid flight phase, and the jet could directly head onto the collector; consequently, a more or less circular section of fiber resulted. The grooved fiber surfaces strongly depended on the ambient humidity, and this has already been covered in many publications.[20–24] It was believed that the temperature on the jet surface descended sharply when the solvent vaporized during the jet flight, and then, the moisture in the wet air around the jet condensed on the jet surface and was arranged in order in the form of water drops. Some ordered honeycomb-like pores appeared on the fiber surfaces after the solvent and drops were vaporized completely. The idea may also have been applicable in this work.

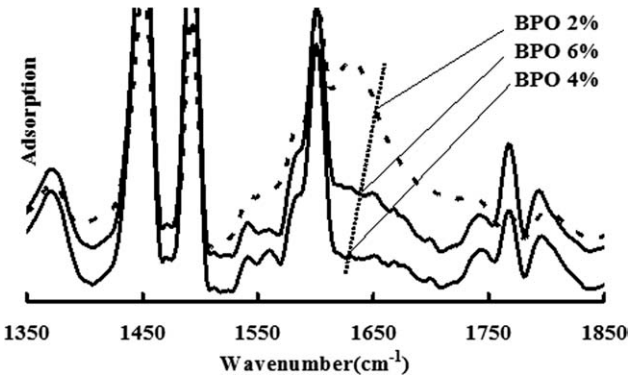

Figure 5. IR spectra of the grafted membranes at different initiator dosages.

What should be emphasized here is that, the fiber surface morphology may signpost the feasibility of the grafting copolymerization with the embedded initiator. As mentioned previously, the smooth ribbonlike fiber surface was caused by rapid solvent evaporation; meanwhile, the rapid evaporation carried little initiator to emigrate toward the fiber surface. The presence of less initiator on the fiber surface gave rise to more scarce grafting. However, the cucumber-skin fiber surface structure, which implied a slow solvent evaporation and then a sufficient amount of initiator emigration, induced the abundant grafting of the copolymers onto the fiber surface. Figure 2 gives the XPS spectra of C_{1s} and O_{1s} of the electrospun fibrous membranes at different RHs. At low humidities, the sharp peak at about 284.6ev was attributed to the C_{1s} of C═C from the phenyl ring and C—C from the skeleton of polystyrene, whereas the outspreading and blueshifting peak indicated the presence of the initiator component at high humidities, the C_{1s} componential peaks of the C═O, and C—O from the initiator–BPO. This complied with the literature.[26] The O_{1s} peak at about 532.2ev was attributed to oxygen atoms, such as S═O and S—O, from the polymer chain end, the initiator residue of potassium persulfate,

Table II. Water Contact Angles on the Membrane Surfaces

Membrane	Water contact angle (°)
1% BPO, ungrafted	135.25
1% BPO, grafted	80.85
6% BPO, grafted but crosslinked	0
8% BPO, grafted but crosslinked	0

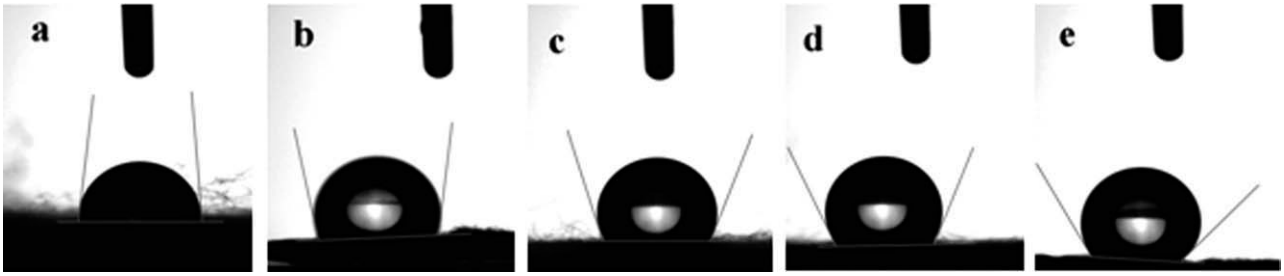

Figure 6. Water contact angles of the grafted membranes at different initiator dosages. The BPO contents and contact angles were as follows: (a) 1% and 80.85°, (b) 2% and 99.25°, (c) 4% and 111.00°, (d) 6% and 116.45°, and (e) 7% and 121.70°.

and the surfactant introduced during emulsion polymerization. The bilateral outspreading peak was attributed to the oxygen atoms of C═O in the low-energy wing and to the oxygen atoms of C—O and the peroxyl O—O in the high-energy wing from the embedded initiator at a high humidity. Therefore, the initiator involved in the dope preparation was finally exiled with the elaborate solvent butanone and favorable humidity during electrospinning, and this circumvented the radical initiation happening on the fiber surface; instead, it happened with the polymer phase-separation technique.[19] This will be really a facile and feasible robust platform for realizing the surface modification of electrospun fibers.

Grafting copolymerization with the initiator present on the fiber surface

Figure 3 displays the infrared spectra of the electrospun fibrous mats and indicates the effective initiation polymerization of the emigrated initiator on the fiber surface. A striking difference was observed in the region 1400–1800 cm^{-1}. The ungrafted sample was a raw membrane with initiator on its surface, and the samples prepared at humidities of 20 and 40% were grafted at a BPO concentration of 30% v/v. There existed an extremely small amount of acidic groups, as indicated by the twin bands of 1770 and 1800 cm^{-1}. These two bands are usually considered to be C═O stretching vibrations in very dilute solutions in nonpolar solvents.[27] In this situation, the scarcely scattered poly(acrylic acid) chains would have hopelessly been on the membrane surface. However, the sample prepared at a humidity of 70% gave much stronger adsorptions in the region 1550–1750 cm^{-1}, at about 1550 and 1425 cm^{-1}. The adsorptions in the region 1550–1750 cm^{-1} were thought to be due to plenty of carboxylic groups present, namely, the adsorption of hydrogen bonds and/or the dimers of acidic groups, whereas the bands at 1550 and 1425 cm^{-1} were assigned to asymmetric and symmetric stretching, respectively, of the ionized carboxylic group. In conclusion, the abundant amount of initiator expelled onto the fiber surface really initiated copious grafting polymerization at a high humidity.

Table I lists the water uptake of the grafted membranes prepared at different RHs. The membranes made at a high humidity adsorbed more water than those made at a low humidity, and the effect of the humidity on the water uptake seemed to be less important at RHs higher than 60%. Naturally, a higher water uptake meant more plentiful grafting because of more abundant initiator gathering on the fiber surface.

Figure 4 shows the morphology of the membranes before and after they were grafted. The coarse but stiff fiber surface, as shown Figure 4(a), may have implied the enrichment of the initiator on the fiber surface, and this ensured subsequent radical grafting. The rigid fiber appearance was the result of the drawing of electric force, and recent measurement with small-angle neutron scattering techniques showed that polystyrene was a bit more extended in the fiber axis than in perpendicular direction.[28] The swollen and sluggish wrinkle fiber surface indicated fiber enwrapping with grafted poly(acrylic acid), as shown in Figure 4(b). The sectional image of the fiber did show the

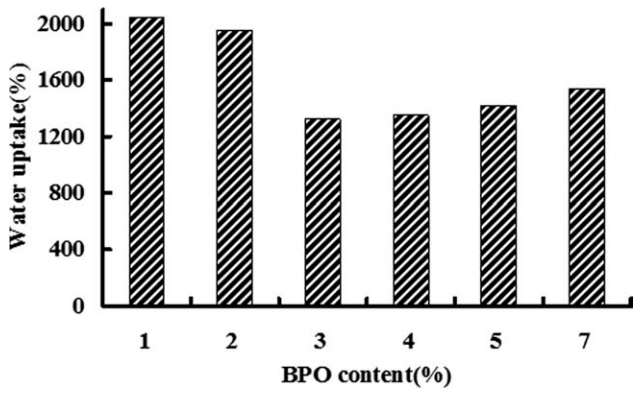

Figure 7. Water uptake of the membranes grafted at different initiator dosages.

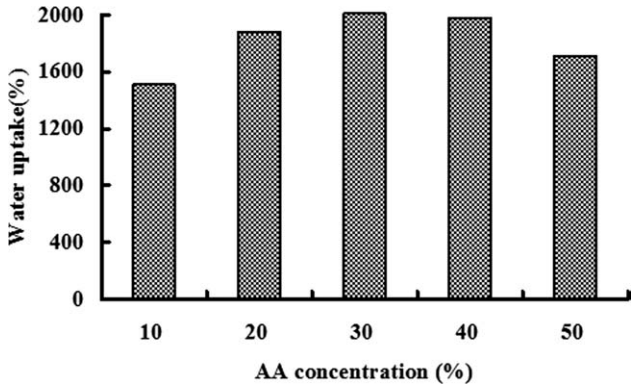

Figure 8. Water uptake of the membranes grafted at different BPO concentrations (BPO concentration = 4%, and the monomer was not neutralized).

Table III. Water Contact Angles of the Membranes Grafted at Different BPO Concentrations

BPO concentration (% v/v)	10	20	30	40	50
Water contact angle (°)	93.85	106.85	108.80	110.75	105.75

enclosure of the fibers, as indicated in the oval areas in Figure 4(c) (noted in the circles). On the basis of these images, the thickness of the enwrapping layer was about 0.2 μm when the moisture-imbibed expansion was neglected, the densities of grafting and polystyrene were assumed to be same, and the maximum grafting yield was about 32 wt % (the monomer concentration at 30% v/v); in comparison, the grafting yield for the electrospun poly(ethylene terephthalate) nanofibers was about 2.2 wt % with Ce(IV) initiated at an MAA concentration of 10% v/v at 80°C for 100 min.[17]

Effect of the initiator dosage

Figure 5 demonstrates the effect of the initiator dosage on grafting. The twin bands at 1770 and 1800 cm^{-1} came from the single carboxylic group for the membranes at an initiator dosage of 4%, whereas the membrane at an initiator dosage of 2% presented a much strong adsorption in the region 1550–1750 cm^{-1}, and the adsorptions implied many more carboxylic groups attached in the membranes, as mentioned previously. In addition, the adsorption bands at 1425 and 1550 cm^{-1} were also assigned to the asymmetric and symmetric stretching of ionic carboxylic groups. This indicated that a lower dosage of the initiator gave rise to more abundant grafting. Generally, the higher the initiator content is, the more quickly the polymerization will proceed. The fluffy and swollen fibrous membranes after grafting will adsorb more monomer and even present viscous and somewhat thermal insulation features. In this case, the rapid polymerization may soon lead to the autoacceleration of polymerization. The consequence of autoacceleration happening in solution inversely deteriorates the grafting yield.

Table II shows the water contact angles of the different membranes. The membrane embedded with initiator gave a water contact angle of 135.25°; this indicated the hydrophobic nature

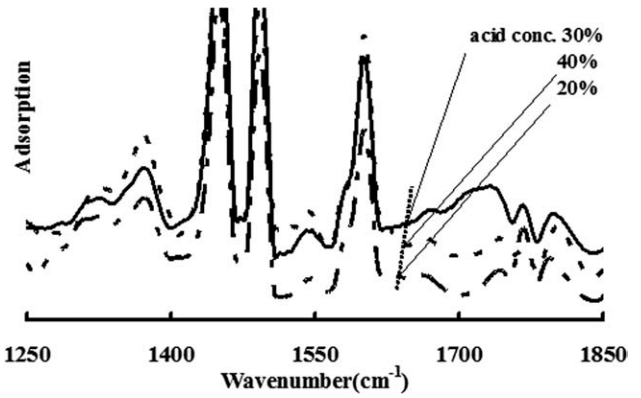

Figure 9. IR spectra of the membranes grafted at different BPO concentrations.

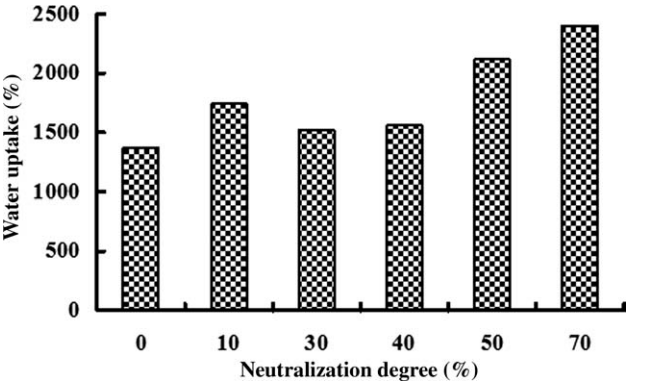

Figure 10. Water uptake of the membranes grafted at different neutralization degrees.

of the original polystyrene. The contact angle immediately decreased to 80.85° after the membrane was grafted at a dosage of 1% simply because of the grafted hydrophilic poly(acrylic acid). The contact angles of the membranes grafted with initiator dosages of 6 and 8% for 2 h surprisingly become zero. This was thought to be the consequence of crosslinking due to the presence of an excess amount of initiator; this led to autoacceleration and gelation. Namely, only crosslinked polyelectrolytes will show such super water adsorption phenomena.

Figure 6 presents the water contact angles of the membranes at the different initiator dosage. An increase in the initiator content resulted in an increase in the contact angles. The reason was that the higher the initiator dosage was, the larger the propensity for crosslinking was. As a result, fewer poly(acrylic acid) chains were attached to the membranes at a higher dosage.

Figure 7 indicates the water uptake capacity of the membranes. Similarly, the membranes grafted at low initiator dosages possessed better hydrophilicity than those grafted at high dosages. The slight increase in the water uptake capacity of the membranes at initiator dosages of 5 and 7% may have been related to crosslinking that happened at the inside of the membranes because crosslinking is thought to start from the core rather than the skin layers. This apparently promoted the water uptake capacity of the membranes. It should be pointed out that the high water uptake capacity seemed not to correspond well with the large contact angle for the grafted membranes. To our knowledge, there was a very large porosity, about 80%, and, together with the small fiber diameter of about 2–3 μm for the membranes, this feature apparently made the grafted membranes hydrophobic (viz., the porous membranes should be considered as the composite system in the light of the Cassie–Baxter model). In fact, many publications have indicated the superhydrophobic nature of electrospun polymers.[23,29] On the other hand, it is the microporous feature that exaggerated the water uptake because of a wicking effect.

Table IV. Water Contact Angles of the Membranes at Different Neutralization Degrees

Neutralization degree (%)	40	50	70	90
Water contact angle (°)	108.15	106.35	103.20	78.35

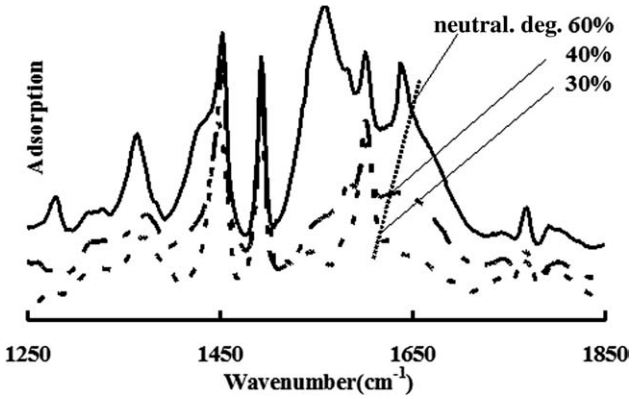

Figure 11. IR spectra of the membranes grafted at the different neutralization degrees.

Concentration and neutralization degree of the monomer

Figure 8 shows the water uptake of the membranes grafted at different monomer concentrations. The water adsorption presented slightly complicated behavior, namely, an initial increase and then a decrease in water uptake with concentration. The implication was that the most copious amount of polyacrylic chains was grafted onto the membranes at a concentration of 30% v/v. Generally, the polymerization rate, the polymerization kinetic chain length, and the grafted polymer molar mass and, thus, water uptake increase with increasing BPO concentration. As mentioned before, the increase in the polymerization rate may have easily led to the autoacceleration and gelation processes, especially for the nonneutralization monomer. The gelation inversely gave rise to a small amount of polyacrylic chains to be pended onto the membranes. BPO at about 30% v/v is usually thought to be the critical concentration to show up the gelling process.

Table III gives water contact angles of the membranes grafted at different monomer concentrations. Again, the contact angle presented totally different behavior, with a slight increase with monomer concentration, in contrast to the water uptake behavior. This may still have stemmed from the crosslinking and gelation processes. The crosslinked polyelectrolyte inside the core may have given a high water uptake but one that was not right for the contact angle because the contact angle mainly responded to the surface nature. The gelation process originating from the core layers spread out to the whole solution. The crosslinked and grafted polyacrylic substance could be peeled off manually from the membrane surface, but a trace amount of the crosslinked structure may still have stayed at the core layers. In this case, the bulky water uptake but highly hydrophobic membrane surface appeared simultaneously.

In Figure 9, the adsorption band at 1770 cm^{-1} for the membrane grafted at 20% v/v was ascribed to the C=O stretching of a single acidic group. Although the sample grafted at 30% included many more carboxylic groups, as indicated in the region 1700–1740 cm^{-1}, coming from hydrogen-bonded acidic groups, interestingly, the sample at 40% indicated adsorption due to a cluster of ionic carboxylic groups, as shown for asymmetric stretching at 1546 cm^{-1} and symmetric stretching at 1373 cm^{-1}. This again meant that more abundant carboxylic groups were attached at higher concentrations. However, the membrane grafted at 50% did not show strong adsorption, as did those grafted at concentrations of 30 and 40%. This implied that plenty of monomer was not grafted onto the membrane but formed a crosslinked homopolymer (the spectra grafted at 50% is not shown in Figure 10).

Figure 10 presents the relationship between the water uptake and the neutralization degree of the monomer. Surprisingly, the water uptake showed an almost linear relationship with the neutralization degree; this was totally different from the behaviors of monomer concentration and initiator dosage. The neutralization of AA usually diminishes the polymerization rate by restraining the monomer diffusion because of the involved electrostatic interaction, and this reduces the probability of autoacceleration polymerization.[30] The reduction of the polymerization rate will cause a high polymer molar mass and, thereby, good water uptake. Table IV demonstrates the water contact angles of the membranes at different neutralization degrees. The increase in neutralization gradually led to a decrease in the water contact angle and, namely, an improvement in the hydrophilicity of the grafted membranes.

Figure 11 shows the infrared spectra of the membranes grafted at different neutralization degrees, and the grafting difference was also indicated by adsorptions in the regions of 1360, 1550, and 1600–1800 cm^{-1}. The three regional adsorption features were all explained previously. Conclusively, more abundant carboxylic groups were attached at higher neutralization degrees.

CONCLUSIONS

The electrospinning and surface-grafting modification of polystyrene fibrous membranes were carried out via the embedded radical initiator approach. The initiator was deliberately expelled onto the fiber surface by manipulation of the electrospinning conditions. The increase in the initiator dosage led to decreases in the grafting, water uptake, and hydrophilicity, whereas the enhanced neutralization of AA improved the grafting, water uptake, and surface hydrophilicity of the grafted membranes. The grafting, water uptake, and hydrophilicity presented nonlinear relationships with AA. The high water uptake capacity did not correspond to the large contact angle due to the crosslinking and gelation processes happening at the inner layer and the microporous structural features. The emigrating initiator technique will provide a facile and feasible platform for the surface-grafting modification of electrospun nanofiber membranes.

ACKNOWLEDGMENTS

This work was partly financially supported by the First Phase of Jiangsu Universities' Distinctive Discipline Development Program for Textile Science and Engineering of Soochow University.

REFERENCES

1. Zhu, Y.-B.; Leong, M. F.; Ong, W. F.; Chan-Park, M. B.; Chian, K. S. *Biomaterials* **2007,** *28*, 861.
2. Ma, Z.; Kotaki, M.; Ramakrishna, S. *J Membr Sci* **2006,** *272*, 179.

3. Barhate, R. S.; Ramakrishna, S. *J Membr Sci* **2007,** *296*, 1.
4. Patel, A. C.; Li, S.-X.; Wang, C.; Zhang, W.-J.; Wei, Y. *Chem Mater* **2007,** *19*, 1231.
5. Wang, X.-F.; Ding, B.; Yu, J.-Y.; Wang, M.-R.; Pan, F.-K. *Nanotechnology* **2010,** *21*, 055502.
6. Neghlani, P. K.; Rafizadeh, M.; Taromi, F. A. *J Hazard Mater* **2011,** *186*, 182.
7. Huang, X.-J.; Chen, P.-C.; Huang, F.; Ou, Y.; Chen, M.-R.; Xu, Z.-K. *J Mol Catal B* **2011,** *70*, 95.
8. Cécile, C.; Hsieh, Y.-L. *J Appl Polym Sci* **2009,** *113*, 2709.
9. Uyar, T.; Havelund, R.; Hacaloglu, J.; Zhou, X.-F.; Besenbacher, F.; Kingshott, P. *Nanotechnology* **2009,** *20*, 125605.
10. Teoh, S. H.; Chen, F.; Lee, C. N. *Mater Sci Eng C* **2007,** *27*, 325.
11. Wei, Q.-F.; Gao, W.-D.; Hou, D.-Y.; Wang, X.-Q. *Appl Surf Sci* **2005,** *245*, 16.
12. Martins, A.; Pinho, E. D.; Faria, S.; Pashkuleva, I.; Marques, A. P.; Reis, R. L.; Neves, N. M. *Small* **2009,** *5*, 1195.
13. Yao, C.; Li, X.-S.; Neoh, K. G.; Shi, Z.-L.; Kang, E. T. *Appl Surf Sci* **2009,** *255*, 3854.
14. Kaur, S.; Ma, Z.; Gopal, R.; Singh, G.; Ramakrishna, S.; Matsuura, T. *Langmuir* **2007,** *23*, 13085.
15. Park, K.; Ju, Y.-M.; Son, J.-S.; Ahn, K.-D.; Han, D.-K. *J Biomater Sci Polym Ed* **2007,** *18*, 369.
16. Shin, Y.-M.; Shin, H.-S.; Lim, Y.-M. *Macromol Res* **2010,** *18*, 472.
17. Ma, Z.; Kotaki, M.; Yong, T.; He, W.; Ramakrishna, S. *Biomaterials* **2005,** *26*, 2527.
18. Ma, Z.; Ramakrishna, S. *J Appl Polym Sci* **2006,** *101*, 3835.
19. Liu, X.; Yang, D.-Y.; Jin, G.; Ma, H.-W. *J Mater Chem* **2010,** *20*, 10228.
20. Park, J.-Y.; Lee, I.-H. *J Nanosci Nanotechnol* **2010,** *10*, 3473.
21. Medeiros, E. S.; Mattoso, L. H. C.; Offeman, R. D.; Wood, E. F.; Orts, W. J. *Can J Chem* **2008,** *86*, 590.
22. Zhu, X.-S.; Jiang, X.-S.; Cheng, S.; Wang, K.; Mao, S.-L.; Fan, L.-J. *J Polym Res* **2010,** *17*, 769.
23. Lin, J.-Y.; Ding, B.; Yu, J.-Y.; Hsieh, Y.-L. *Am Chem Soc Appl Mater Interfaces* **2010,** *2*, 521.
24. Casper, C. L.; Stephens, J. S.; Tassi, N. G. *Macromolecules* **2004,** *37*, 573.
25. Teo, W.-E.; Ramakrishna, S. *Compos Sci Technol* **2009,** *69*, 1804.
26. Jin, S.-S.; Shi, Y.; Xu, X.-C. *Chem Res Appl* **2006,** *18*, 943.
27. Socrates, G. Infrared Characteristic Group Frequencies, Tables and Charts, 2nd ed.; Wiley: Chichester, United Kingdom, **1994; p 90.**
28. Mohan, S. D.; Mitchell, G. R.; Davis, F. J. *Soft Matter* **2011,** *7*, 4397.
29. Li, X.-H.; Ding, B.; Lin, J.-Y.; Yu, J.-Y.; Sun, G. *J Phys Chem* **2009,** *113*, 20452.
30. Beuermann, S.; Buback, M.; Hesse, P.; Kukučková, S.; Lacík, I. *Macromol Symp* **2007,** *248*, 23.